PROCEEDINGS OF SCIENCE

Influence of Galactic magnetic fields on UHECR energy spectrum and mass composition on the Earth

Ryo Higuchi,[a,*] **Toshihiro Fujii,**[c,d] **Kazumasa Kawata,**[b] **Eiji Kido,**[a] **Shigehiro Nagataki**[a] **and Takashi Sako**[b]

[a] *Astrophysical Big Bang Laboratory, RIKEN, 2-1 Hirosawa, Wako, Saitama 351-0198, Japan*

[b] *Institute for Cosmic Ray Research, The University of Tokyo, 5-1-5 Kashiwanoha, Kashiwa, Chiba 277-8582, Japan*

[c] *Osaka Metropolitan University, 3-3-138 Sugimoto Sumiyoshi-ku, Osaka-shi, 558-8585, Japan*

[d] *Nambu Yoichiro Institute of Theoretical and Experimental Physics, 3-3-138 Sugimoto Sumiyoshi-ku, Osaka 558-8585, Japan*

E-mail: ryo.higuci@riken.jp

Considering source population, mass composition, and propagation in magnetic fields is important to reveal the origin of ultrahigh-energy cosmic rays (UHECRs). Currently, Telescope Array (TA) and Auger experiments have observed the energy spectrum, mass composition, and anisotropy of arrival directions at an ultrahigh-energy scale. On the other hand, the interpretation of these observables is strongly affected by model assumptions. In our previous works, we investigated the effect of the Galactic magnetic field (GMF) on the anisotropy of arrival directions through the analysis of the mock datasets and found that contributions of the starburst galaxy are underestimated. In this study, we apply the technique in previous studies and investigate the effect of GMF on the energy spectrum and mass composition. We especially discuss the discrepancy in energy spectrum between the northern and southern hemispheres reported by the TA and Auger experiments.

38th International Cosmic Ray Conference (ICRC2023)
26 July - 3 August, 2023
Nagoya, Japan

*Speaker

PoS(ICRC2023)460

1. Introduction

Telescope Array (TA) [1] and Auger experiments [2] lead ultrahigh-energy cosmic ray (UHECR) observations in the north and south sky, respectively. The major observational results of these experiments consist of the energy spectrum, mass composition, and anisotropy of arrival directions. The interpretation of these observables is important to constrain the origin of UHECRs.

There is a difference between the energy spectrum between TA and Auger experiments [3, 4]. Generally, the flux of UHECRs with the TA experiment is higher than that of the Auger experiment at all energy bins. Even after rescaling the energies of TA and Auger experiments with ±4.5%, the flux of the TA experiment is higher than that of Auger at higher energy bins.

There are tries to explain the discrepancy of the energy spectrum: the first explanation for the discrepancy is the systematic uncertainties caused by the difference in detectors and reconstruction methods. However, [4] suggests that the difference in analysis methods does not affect the discrepancy between the TA & Auger energy spectrum. The second is an astrophysical origin that causes the discrepancy. For example, [5] suggests the local source in the northern sky, which can explain the higher CR flux of the TA experiment. Another explanation is what we propose in this report: the influence of the magnetic fields on the energy spectrum.

In our previous works, we investigated the effects of the GMF deflection on UHECR anisotropies [6, 7]. The deflection of UHECRs caused by GMF affects the distribution of UHECRs. The limitation of sky coverage of the experiment also affects the analysis of the UHECR anisotropy.

In this study, we investigate the systematic difference in the energy spectrum caused by the Galactic magnetic field (GMF). For the source model, we assume the nearby starburst galaxies reported in [12, 13]. For the model of GMF, we adapt the JF12 model [8, 9] and PT11 model [10].

2. Method

2.1 Dataset generation without photodisintegration process

We mainly follow the dataset generation process in [6, 7]. If we ignore the GMF deflections, the CR flux outside the Galaxy can be written as

$$F_{\rm org}(\mathbf{n},\theta) = \frac{\sum_i f_i \exp(\mathbf{n}_i\cdot\mathbf{n}/\theta^2)}{\int_{4\pi}\sum_i f_i \exp(\mathbf{n}_i\cdot\mathbf{n}/\theta^2)d\Omega}. \tag{1}$$

In this equation, the deflections by EGMF are approximated to be Gaussian smearing with the separation angular scale θ. To reflect the deflection by GMF, we define the backtracked trajectories of CRs as

$$\mathbf{n}_{\rm org} = A_{\rm BT}(\mathbf{n}_{\rm earth}, R), \tag{2}$$

where $A_{\rm BT}$ represents the backtracking calculation through GMF models with CRPropa 3.2 [11]. For GMF models, we adapt JF12[8, 9] and PT11[10] models. The GMF models consist of a regular component and a random component. To focus on the difference at the highest energy bins, we consider only regular components. We rewrite the Equation 1 as

$$\begin{aligned} F_{\rm earth}(\mathbf{n}_{\rm earth},\theta,R) &= F_{\rm org}(\mathbf{n}_{\rm org},\theta) \\ &= F_{\rm org}(A_{\rm BT}(\mathbf{n}_{\rm earth},R),\theta). \end{aligned} \tag{3}$$

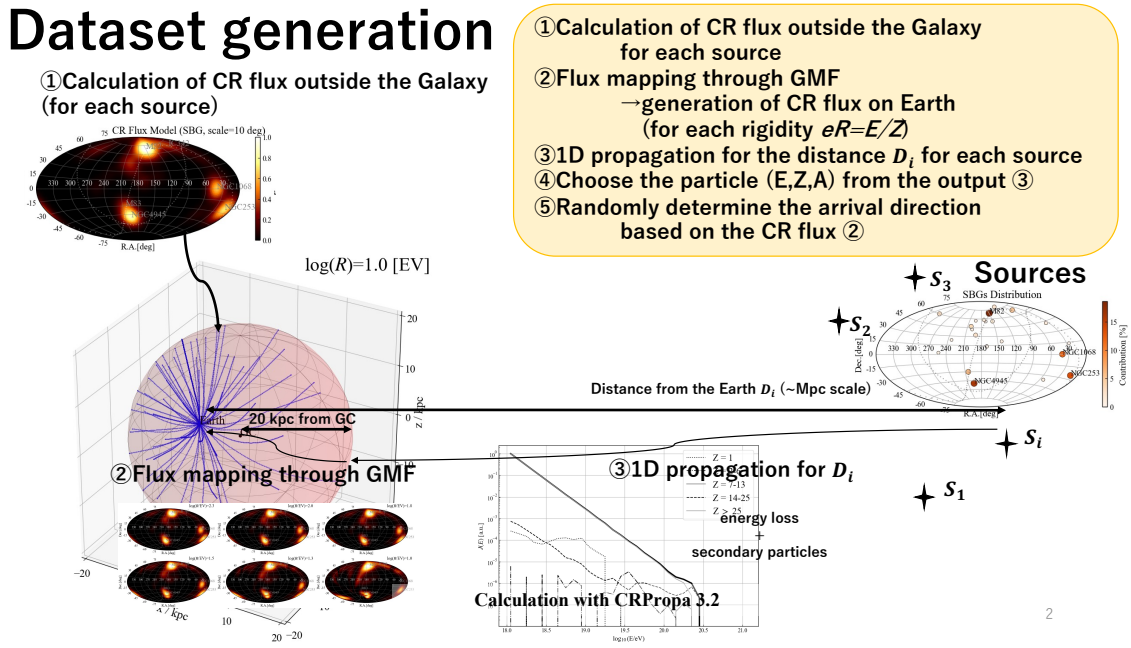

Figure 1: Dataset generation process.

For the energy spectrum on sources, we adapt a power-low spectrum with -2.7 index and single-mass assumption (proton/nitrogen/iron). Although previous UHECR anisotropy studies [12, 13] assume the source contribution (anisotropic fraction) and isotropic backgrounds for UHECRs, we only assume the source contribution.

2.2 Dataset generation with photodisintegration process

To reflect the physical propagation process, we also apply 1-dimensional propagation with CRPropa 3.2 [11]. Figure 1 shows the dataset generation process. We add the 1-dimensional propagation with 10^6 primary CRs and randomly select the events whose energies are above energy thresholds.

We conduct the propagation with the power-low spectrum in Section 2.2. We also test the datasets generated with a mixed-mass assumption [14]. We follow the formulas in [14]:

$$J_A(E) = \mathcal{J}_A f_{\rm cut}(E, Z_A, R_{\rm max}) n_{\rm evol}(z) \left(\frac{E}{10^9\ {\rm GeV}}\right)^{-\gamma}, \tag{4}$$

where $J_A(E)$ is the energy spectrum of each mass (A) on sources, $n_{\rm evol}(z)$ is a redshift evolution term (which is approximated to be 1), and $f_{\rm cut}$ is a cutoff function with maximum rigidity $R_{\rm max}$, respectively. The cutoff function $f_{\rm cut}$ is given as

$$f_{\rm cut} = \begin{cases} 1 & (E < Z_A R_{\rm max}) \\ \exp\left(1 - \frac{E}{Z_A R_{\rm max}}\right) & (E > Z_A R_{\rm max}). \end{cases} \tag{5}$$

Qualitatively the energy spectrum of each mass follows a power-low with an index of $-\gamma$ at lower energies than $Z_A R_{\rm max}$, and follows the exponential cutoff at higher energies than $Z_A R_{\rm max}$. Same as in [6], we adapt the best-fit parameters from [14] as $\gamma = -0.80$ and $R_{\rm max} = 1.6\,{\rm EV}$.

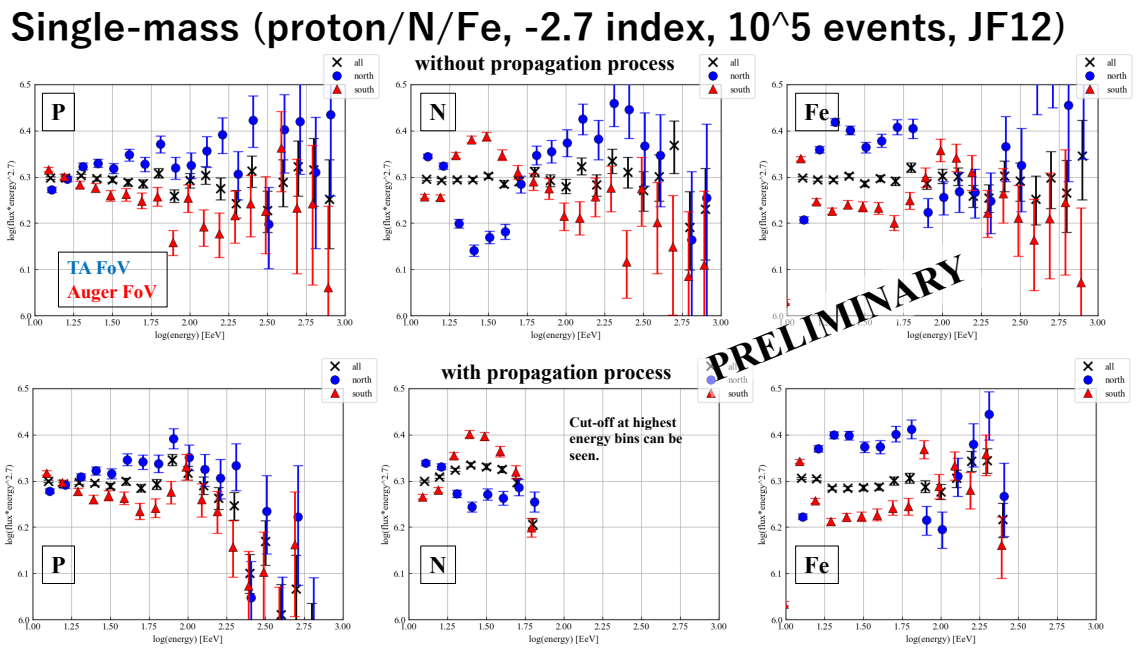

Figure 2: Energy spectrum of mock UHECR datasets with JF12 model. The top and bottom panels show the results without and with the propagation process, respectively. From left to right, each panel indicates single-proton, nitrogen, and iron assumption, respectively. The blue circle (red triangle) represents the results with the FoV of the TA (Auger) experiment.

3. Results and discussions

We show the results in Figures 2 and 3 for JF12 and PT11 models, respectively. In each figure, the top (bottom) panel shows the results with (without) the propagation process. From left to bottom, we assume single-proton, nitrogen, and iron case.

The difference between northern and southern sky largely depends on the regular component of GMF models.

For the JF12 case, the flux with TA sky coverage is larger than that with Auger sky coverage. In the single-nitrogen and iron case, the flux with Auger sky coverage is higher at the rigidity of $\log(eR) \sim 0.6\,\mathrm{EV}$ ($\log(E) \sim 1.5\,\mathrm{EeV}$ for single nitrogen case and $\log(E) \sim 2.0\,\mathrm{EeV}$ for single iron case). This may be because NGC1068 is outside of the TA FoV at this rigidity scale.

For the PT11 case, we can see similar effects as the JF12 case in the single-proton and nitrogen case. In the single-iron case, however, the flux with Auger sky coverage is much larger than that with TA experiment.

The photodisintegration process during the propagation affects the higher energy bins. Especially, the cutoff of the energy spectrum is clearly seen for the single-nitrogen case.

We also show the results for the mixed-mass composition case (photodisintegration process included). Due to the largest contribution of nitrogen, the results is similar to the single-nitrogen case. Below the cutoff of the spectrum, the flux of Auger is slightly higher than TA. At the highest energy bins, the flux of TA is larger than Auger. This is due to the energy loss of CRs from NGC1068 (for example, UHECRs whose energies are above 200 EV cannot reach the earth over

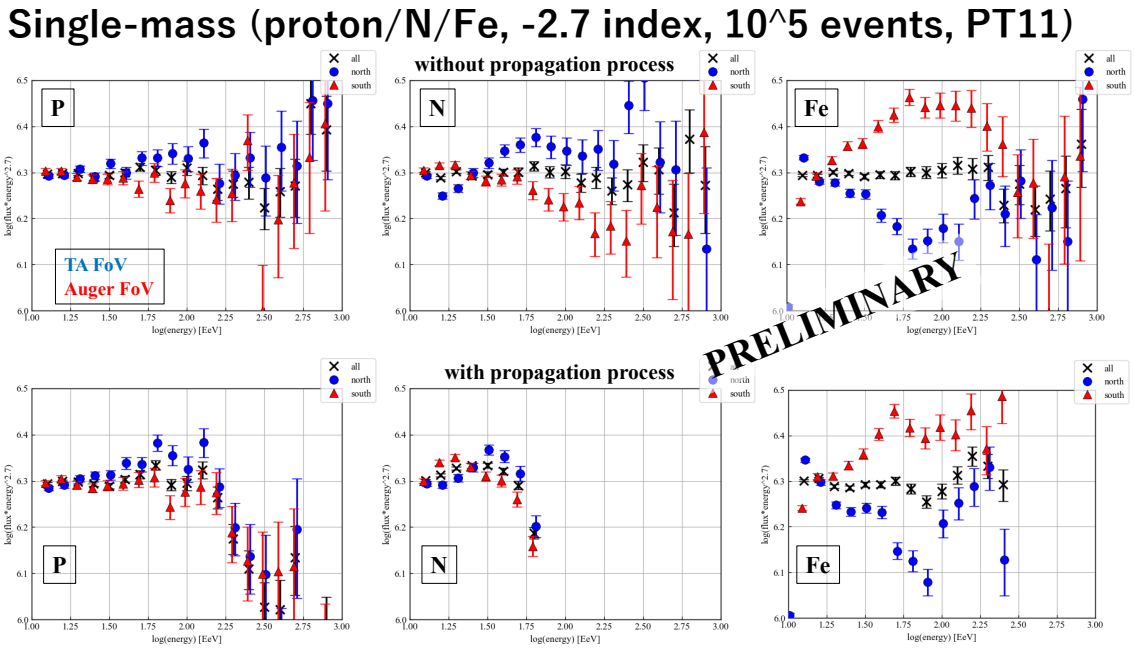

Figure 3: Same as Figure 2, but with PT11 model.

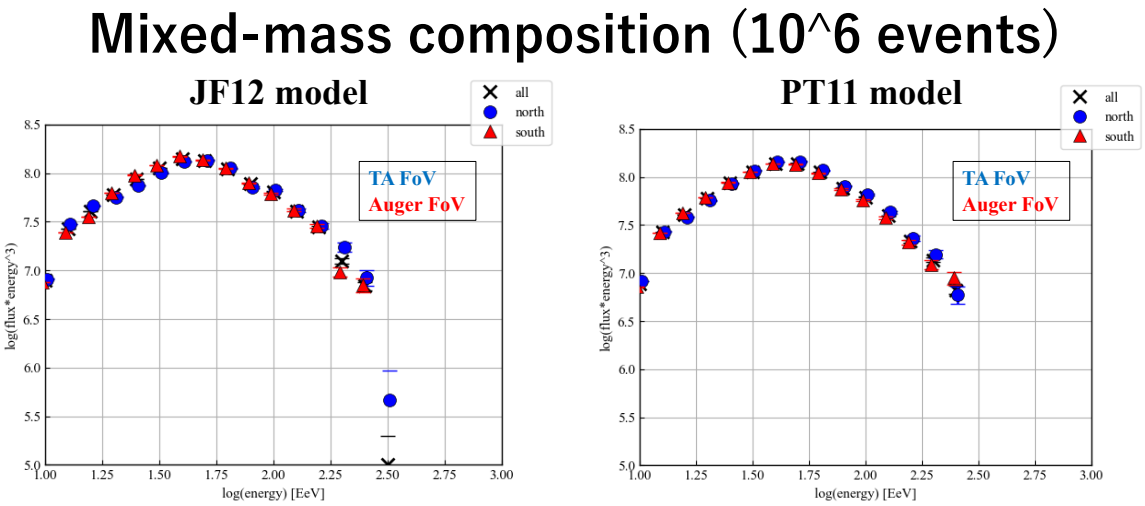

Figure 4: Energy spectrum of mock UHECR datasets with mixed-mass assumption. The left panel and right panels indicate the JF12 model and PT11 models, respectively.

the ∼ 18 Mpc distance).

Although we can see the slight difference between TA and Auger sky coverage for the mixed-mass composition case, it does not explain all the differences between TA and Auger energy spectrum.

4. Summary

In this study, we investigate the systematic difference in the energy spectrum between TA and Auger experiments caused by the Galactic magnetic field (GMF).

Depending on the GMF model and the position of most contributed sources, the effects of GMF appear differently.

Especially when we care the photodisintegration process, the position of NGC1068 is important to the higher energy bins due to the large contribution and larger distance from the earth.

Although we can see the slight difference between TA and Auger sky coverage for the mixed-mass composition case, the deflection by GMF does not explain all the differences between TA and Auger energy spectrum.

We need to note that our assumptions and models are very simple and not realistic. Although we assume 100% contribution of nearby SBGs to UHECRs, [12] suggests only $\sim$ 10% of UHECRs can be explained by the SBGs. When we discuss the effects of magnetic fields in lower energy bins, we need to consider the random component of GMF models (although we focus on the highest energy bins in this report). The scattering by EGMF also needs to be energy-dependent: not like simple Gaussian scattering as in this study.

We also need to note that we assume the same energy spectrum and mass composition for all the SBGs. Especially, the shape of energy spectra of top-4 contributed SBGs (M82, NGC4945, NGC253, and NGC1068) should affect the difference in energy spectrum between TA and Auger experiments. For this scenario, we need to closely look at the astronomical origin considering the GMF deflections.

Acknowledgments

We thank the members of the Telescope Array collaboration for fruitful discussions.

References

[1] Kawai, H., et al. 2008, Nuclear Physics B Proceedings Supplements, 175, 221

[2] Aab, A., et al. 2015a, Nuclear Instruments and Methods in Physics Research, Section A: Accelerators, Spectrometers, Detectors and Associated Equipment, 798, 172

[3] Tsunesada, Y., et al. Joint analysis of the energy spectrum of ultra-high-energy cosmic rays as measured at the Pierre Auger Observatory and the Telescope Array. In Proceedings of 37th International Cosmic Ray Conference — PoS(ICRC2021), volume 395, page 337, 2021.

[4] Bergman, D. R., et al. he energy spectrum of ultra-high energy cosmic rays measured at the pierre auger observatory and the telescope array. EPJ Web Conf., 283:02003, 2023.

[5] Pavlo Plotko, Arjen van Vliet, Xavier Rodrigues, and Walter Winter. Indication of a Local Source of Ultra-High-Energy Cosmic Rays in the Northern Hemisphere. arXiv e-prints, page arXiv:2208.12274, August 2022.

[6] Ryo Higuchi et al 2023 ApJ 949 107

[7] Ryo Higuchi, Takashi Sako, Toshihiro Fujii, Kazumasa Kawata, and Eiji Kido. Estimation and reduction of the biases by the galactic magnetic field on the UHECR correlation studies. In European Physical Journal Web of Conferences, volume 283 of European Physical Journal Web of Conferences, page 03011, October 2023.

[8] Ronnie Jansson and Glennys R. Farrar. Anewmodel of the galactic magnetic field. Astrophysical Journal, 757, 2012.

[9] Ronnie Jansson and Glennys R. Farrar. The galactic magnetic field. Astrophysical Journal Letters, 761:1–5, 2012.

[10] M. S. Pshirkov, P. G. Tinyakov, P. P. Kronberg, and K. J. Newton-McGee. Deriving the Global Structure of the Galactic Magnetic Field from Faraday Rotation Measures of Extragalactic Sources. , 738(2):192, September 2011.

[11] Rafael Alves Batista, Andrej Dundovic, Martin Erdmann, Karl Heinz Kampert, Daniel Kuempel, Gero Müller, Guenter Sigl, Arjen Van Vliet, David Walz, and Tobias Winchen. Crpropa 3 - a public astrophysical simulation framework for propagating extraterrestrial ultra-high energy particles. Journal of Cosmology and Astroparticle Physics, 2016, 2016.

[12] A. Aab et al. An indication of anisotropy in arrival directions of ultra-high-energy cosmic rays through comparison to the flux pattern of extragalactic gamma-ray sources. The Astrophysical Journal, 853:L29, 2018.

[13] R. U. Abbasi et al. Testing a reported correlation between arrival directions of ultra-high-energy cosmic rays and a flux pattern from nearby starburst galaxies using telescope array data. The Astrophysical Journal, 867:L27, 2018.

[14] Heinze, J., & Fedynitch, A. 2019, The Astrophysical Journal, 873, 88